Urban Climate 40 (2021) 100983

Contents lists available at ScienceDirect

Urban Climate

journal homepage: www.elsevier.com/locate/uclim

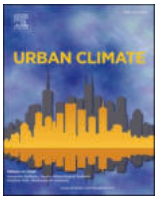

Assessing current and future heat risk in Dublin city, Ireland

Roberta Paranunzio [a], Edward Dwyer [b], James M. Fitton [b], Paul J. Alexander [c], Barry O'Dwyer [b,*]

[a] National Research Council of Italy, Institute of Atmospheric Sciences and Climate (CNR-ISAC), Torino, Italy
[b] MaREI Centre, Environmental Research Institute, University College Cork, Cork, Ireland
[c] Central Statistics Office (CSO), Census Geography, Swords, Dublin, Ireland

ARTICLE INFO

Keywords:
Heat risk
Socioeconomic vulnerability
Climate adaptation
Urban climate
Urban Heat Island
Universal thermal climate index

ABSTRACT

Populations in high-density urban areas are exposed to higher levels of heat stress in comparison to rural areas. New spatially explicit approaches that identify highly exposed and vulnerable areas are needed to inform current urban planning practices to cope with heat hazards. This study proposes an extreme heat stress risk index for Dublin city across multiple decades (2020s–2050s) and for two representative concentration pathways (RCPs). In order to consider the interactions between greenhouse gas emissions and urban expansion, a climate-based urban land cover classification and a simple climate model have been combined to compute air temperature values accounting for urban heat island effect. This allowed the derivation of an improved hazard indicator in terms of extreme heat stress which, when integrated with information on current levels of vulnerability (i.e., socioeconomic factors assessed using principal component analysis (PCA), provides a heat hazard risk index for Dublin city at a fine spatial scale. Between the 2020s and 2050s, urban areas considered at highest risk are expected to increase by about 70% and 96% under RCP 4.5 and 8.5 respectively. For the 2050s, enhanced levels of heat risk under the RCP 8.5 scenario are particularly visible in the core city centre and in the northern and western suburbs. This study provides a valuable reference for decision makers for urban planning and provides an approach to help prioritise management decisions for the development of heat resilient and sustainable cities.

1. Introduction

The frequency of heat extremes and heatwaves in Europe have increased considerably over the last 50 years and in particular since 2000 (European Environment Agency, 2019). Climate change is expected to further increase the intensity, frequency and duration of heatwaves compared to the historical climate (IPCC, 2014; Guerreiro et al., 2018). Recent heat wave events, like the eastern European/Russian heat-wave in 2010 (Barriopedro et al., 2011; Pappenberger et al., 2015), the summer heatwave 'Lucifer' in 2017 and the 2003 European heatwave with more than 70,000 victims (Robine et al., 2008), have highlighted the health-related impacts of heatwaves across Europe and particularly for those populations considered most vulnerable.

In this context, large cities are of particular concern (Zhou et al., 2015); this is because local climate warming is exacerbated by urban areas when compared to their surrounding rural locations, a phenomenon known as the Urban Heat Island effect (UHI). The

* Corresponding author.
E-mail addresses: r.paranunzio@isac.cnr.it (R. Paranunzio), ned.dwyer@randbee.com (E. Dwyer), james.fitton@ucc.ie (J.M. Fitton), paul.alexander@cso.ie (P.J. Alexander), B.ODwyer@ucc.ie (B. O'Dwyer).

https://doi.org/10.1016/j.uclim.2021.100983
Received 26 April 2021; Received in revised form 6 August 2021; Accepted 10 September 2021
Available online 5 October 2021

effects of UHIs on warming of urban areas has been assessed considering both surface and air temperature observations (Arnfield, 2003; Chakraborty et al., 2020; Imhoff et al., 2010; Li et al., 2017; Oke, 1982; Oke et al., 2017; Peng et al., 2012; Zhao et al., 2014). The UHI effect has been shown to contribute to increased levels of heat stress and mortality among vulnerable populations (Chapman et al., 2017; Gasparrini et al., 2017; Guo et al., 2017; Mallen et al., 2019; Santamouris, 2020). Cities concentrate key infrastructure and large populations including many who may be elderly, poor or suffer economic and social deprivation and are therefore more vulnerable to the adverse effects of extreme heat (European Environment Agency, 2019). Additionally, extreme heat also increases energy demand for warm season cooling, impacts on water demand, exacerbates air pollution and puts additional pressure on infrastructure (IPCC, 2014). As a result, for urban areas, especially those that are densely populated and of a size that they influence their micro-climate (IPCC, 2014; Paranunzio et al., 2019), projecting the effects of climate change on heat-related risks is considered critical to support adaptation to climate change impacts.

In Ireland, observed changes in the climate over the last century are in line with global and regional trends associated with human induced climate change (Cámaro García and Dwyer, 2021). Mean surface air temperatures have risen by approximately 0.9 °C since 1900 with heatwave events reported for 1983, 1984, 1995, 2003, 2006, 2018 and 2021. Over the coming decades, increases in both mean surface air temperatures and in the frequency and intensity of heatwaves are expected with up to 15 heatwaves (considered as periods of more than three consecutive days exceeding the 99th percentile of the daily maximum temperature of the May to September season of the control period (1981–2000)) projected over the period 2041–2060 (Nolan and Flanagan, 2020).

For Ireland, heatwaves are currently rare but have been associated with increases in mortality, with levels of heat-related mortality and morbidity shown to increase in the days following the exposure to heatwaves and with higher increases reported for urban areas

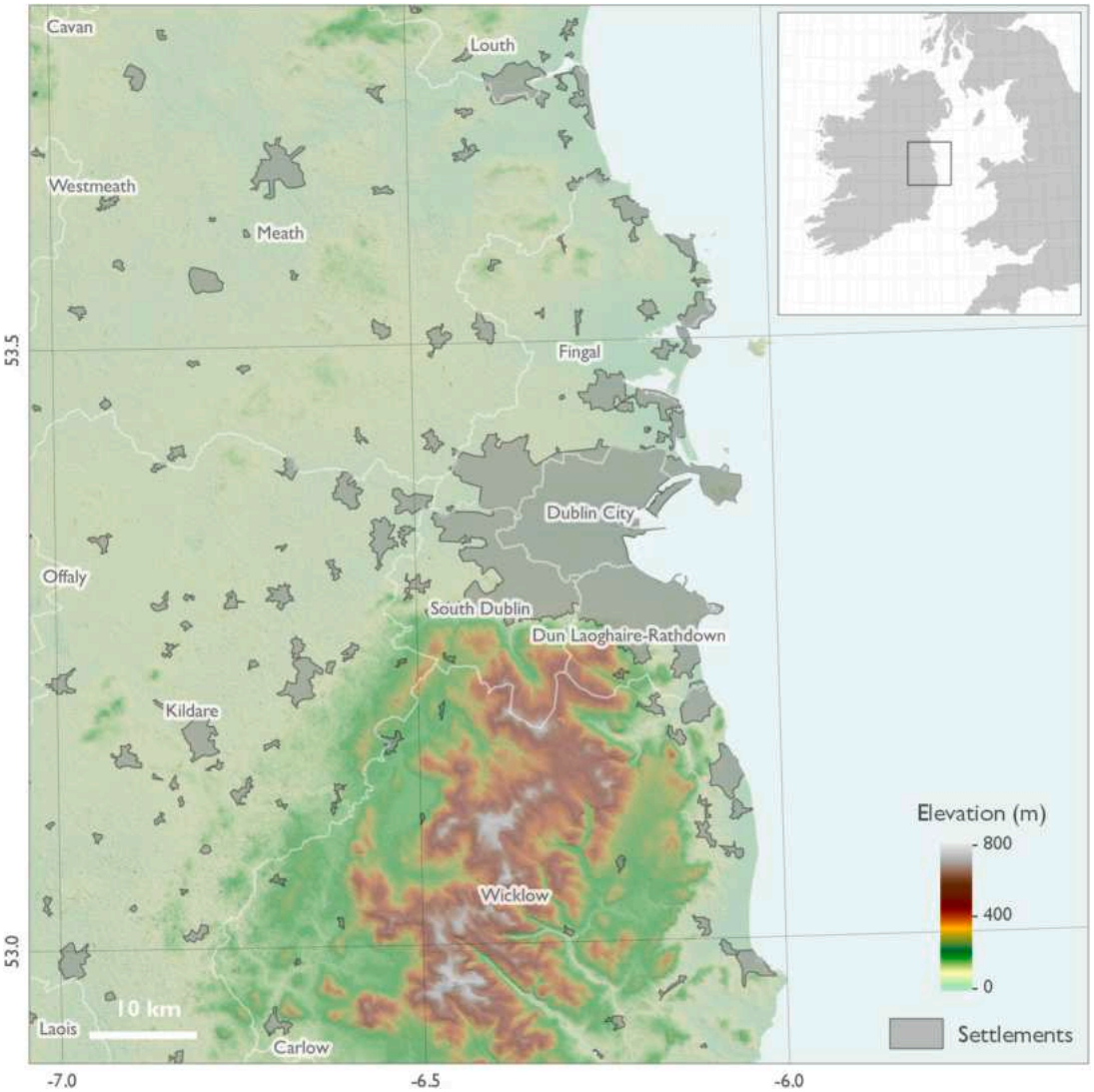

Fig. 1. Map of the modelled region of interest. Settlement data from the Central Statistics Office (CSO, 2019b).

(Barnett et al., 2009). Although rare events, heatwaves and heat-related risks still need to be considered as a climate change related health challenge in temperate climate countries like Ireland (Paterson and Godsmark, 2020). As a result, projected increases in the frequency of heatwaves is likely to increase health-related impacts and this is compounded by Ireland's demographic characteristics and patterns of planned development. Ireland's population is considered to be ageing faster than other parts of Europe and this is expected to result in increased levels of heat related risks for Ireland (CSO, 2019a; Nolan and Flanagan, 2020). Moreover, Project Ireland 2040 which outlines the national development strategy aims to deliver compact and sustainable growth with a focus on further developing existing urban areas including Ireland's 5 major cities and urban centres. Without appropriate heat mitigation and adaptation, this has the potential to exacerbate the UHI effect.

Scientific assessments concentrating on the mapping of heat-risk which includes exposure and vulnerability factors are increasing worldwide (Ellena et al., 2020; Estoque et al., 2020; Georgiadis, 2017; Hatvani-Kovacs et al., 2016; Hua et al., 2021; Navarro-Estupiñan et al., 2019; Sabrin et al., 2020). To date, in Ireland, research has focussed primarily on risks associated with changing patterns of precipitation and sea level rise but little attention has been given to heat-related risks for Ireland's urban areas (Paterson and Godsmark, 2020). On a global basis, vulnerability to heat risk has been found to be associated with a range of factors including

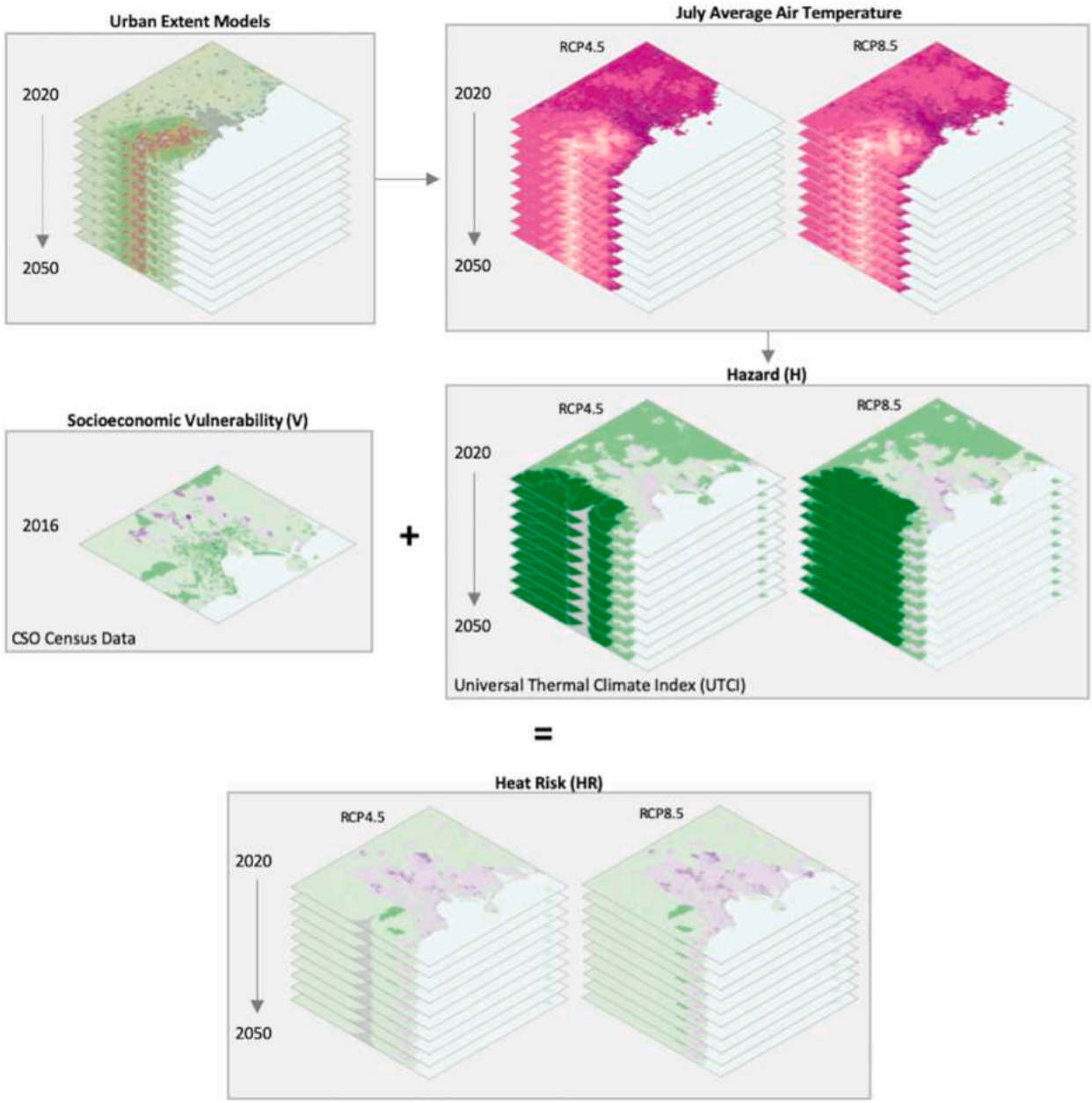

Fig. 2. Workflow of the modelling chain applied to obtain the integrated spatial Extreme Heat Risk index.

socioeconomics, demographic, social isolation status and building conditions (Chow et al., 2012; Ellena et al., 2020; O'Malley, 2007) with some common factors also being identified for Ireland (Paterson and Godsmark, 2020). To support the assessment of heat risk, it is essential to assess how the climate has been changing while also considering land cover evolution. Indeed, while there are many examples of risk assessments for cities in relation to climate change, most of these studies do not integrate future land cover configurations into their analysis as a measure of enhanced exposure to climate risk as a result of the UHI effect. Recently some authors have focussed on the nexus between urban land cover and land surface temperature in Dublin city and neighbouring urban areas across multiple years (Alexander et al., 2017, 2016; Alexander et al., 2015a, 2015b). Similarly, recent studies for other cities have assessed heat risk at the neighbourhood level in densely populated areas (Maragno et al., 2020; Savić et al., 2018; Verdonck et al., 2019) and some of these have evaluated the impact of urban expansion in terms of Representative Concentration Pathway (RCP, Working Groups I II III and IPCC, 2014) scenarios and Local Climate Zones (LCZ) for current and future periods (e.g., in Brussels city, Verdonck et al., 2019). Moreover, land cover and land surface temperature data are essential to properly model the complex interactions between urban surface and the atmosphere in terms of energy balance under different climate change scenarios (Järvi et al., 2011; Rafael et al., 2017).

This study proposes a comprehensive approach to the integrated assessment of spatiotemporal variations of heat risk for Dublin city, Ireland. By coupling a Local Climate Zones-based land cover and the Surface Urban Energy and Water Balance Scheme (SUEWS) model under different radiative forcing scenarios and across time periods (Alexander et al., 2016; Rafael et al., 2017), population exposure to the hazard of extreme heat stress in terms of the Universal Thermal Climate Index (UTCI, Di Napoli et al., 2018) has been assessed. Employing socio-economic data, the socio-economic vulnerability of the population to heat-related health impacts has been assessed. On this basis, a heat risk index has been developed and mapped to assess current and future heat risk as a function of different total radiative forcing scenarios and modelled land cover changes.

2. Study site

Dublin which is the capital of the Republic of Ireland with a population of about 1.2 million people (Fig. 1) forms the focus of this study. The city is located on the east coast of Ireland, and it is surrounded by the Wicklow mountains to the south and the Irish Sea to the east. The study area occupies a mostly low-lying basin (<200 m a.s.l.). The climate of the region is relatively uniform and is generally characterized as maritime-temperate oceanic (type Cfb according to the modified Köppen-Geiger scheme) with cool winters and mild summers, good moisture availability throughout the year, and few extremes of temperatures. The 30-year climate averages (1981–2010) at Dublin airport show a mean annual temperature of 9.7 °C, and mean annual precipitation of 758 mm (Met Éireann, 2021). Administratively Dublin comprises four local authority areas and is part of the Eastern and Midlands Region Assembly. The extent of the investigated area is approximately 700 km^2 (boundary coordinates: −6.39°, 53.29°: −6.11°, 53.41°) and comprises 2187 small areas as defined by Ireland's Central Statistics Office (CSO). Small areas are the smallest administrative units in Ireland designed for the compilation of statistics in line with data protection and generally comprises either part or complete neighbourhoods or townlands (CSO, 2019b).

3. Material and methods

As defined by the IPCC, risk is considered a function of hazard, exposure, and vulnerability of the population to that hazard (Oppenheimer et al., 2014). Exposure to heat stress or high temperatures also depends on urban morphology (Verdonck et al., 2019). For this reason, changes in urban land cover are often used as a proxy of exposure in heat risk studies. In order to derive a thermal stress indicator which accounts for the effect of urban heat, a modelling approach used in recent studies (Alexander et al., 2016) which incorporates a climate-based land classification and an urban model (SUEWS) under different RCP scenarios has been adopted. The air temperature values derived from this model account for the UHI effect and are used as inputs for the computation of an improved hazard indicator i.e., thermal heat stress (specifically, UTCI), which includes the exposure component itself. This integrated indicator, combined with the current vulnerability component, provides the final Heat Risk index (HR) for each decade and RCP at the small area scale. Fig. 2 shows the workflow adopted in this study. Further details on the modelling chain adopted are detailed hereinafter.

3.1. Heat exposure and hazard – UTCI computation

3.1.1. Land cover projections

Different urban development scenarios could have considerable impacts on the local-scale climate across a city during a typical climatological year (Alexander et al., 2017, 2016). In order to account for the influence of land cover on the climate across Dublin city, models of urban extent have been developed based on CORINE Land Cover (CLC) information (Copernicus Land Monitoring Service, 2021) and for the period 2020s–2050s by means of a Land Change Modeler (LCM). CLC uses a minimum width of 100 m for linear phenomena and a Minimum Mapping Unit (MMU) of 25 hectares (ha) for areal phenomena (European Environment Agency, 2019). Here, the CLC inventory has been modified and tailored to fit the modelling requirements to evaluate climate change impacts. Land cover information for this work has been obtained at a spatial resolution of 30-m from the CLC employing the approach detailed in Alexander and Mills (2014) and Alexander et al. (2016). Subsequently and to support further analysis using the SUEWS model (spatial resolution of 1 km × 1 km), this information has been resampled in a GIS environment to a spatial resolution of 1 km × 1 km. Here, an approach which modifies the CLC inventory to simplify non-urban landcover while maintaining the same level of detail for urban land cover has been employed and 11 land use classes have been identified (4 urban and 7 non-urban classes). The urban land cover classes

are associated with the Local Climate Zones (LCZ) classification (Stewart and Oke, 2012; Verdonck et al., 2018). The LCZ scheme describes neighbourhood types and incorporates the properties of the urban environment that contribute to UHI (Stewart and Oke, 2012). This scheme has been applied to Dublin previously (Alexander and Mills, 2014) and offers the possibility to observe urban temperature effects based on differences between neighbouring cells that include the relevant microclimatic process (Table 1). Further details on the LCZ classification assessment for Dublin city are detailed in previous works (Alexander et al., 2015a, 2015b; Alexander and Mills, 2014; Bechtel et al., 2015).

Future growth scenarios generate distinct land use outcomes, which are translated into LCZ types (Alexander et al., 2017; Alexander and Mills, 2014). For the purposes of projecting future land use, a LCM module in a GIS environment was employed for analysing past land use changes and for generating scenarios of future land use from 2020 up to 2050 (Alexander and Mills, 2014). Historical transitions i.e. time-series of land use maps and a Markov-Chain are used to model forward to user specified dates based on transition potentials. These are informed by predictor variables (e.g. distance to roads, slope of the landscape) and restrictor variables (e.g. proximity to special protected areas or areas designated as flood zones). All the required data were derived in consultation with planners in the Eastern and Midlands Regional Assembly.

3.1.2. Coupling a climate-based land classification and an urban energy budget model

To assess the climatic impact of different urban development pathways, a Land Surface Scheme (LSS)/Urban Energy Budget (UEB) Model called the Surface Urban Energy and Water Balance Scheme (SUEWS) (Järvi et al., 2011) has been employed. Such an approach has already been employed in previous studies (Rafael et al., 2017) and when applied to the Greater Dublin Region (GDR) proved to be able to simulate the effect of urbanization on local climate (Alexander et al., 2016). More specifically, Alexander et al. (2016) used hourly values of meteorological variables recorded by the Dublin Airport WMO standard station to force the SUEWS model over the 2005–2014 period. To ensure good agreement with observations of the urban energy balance (UEB), the turbulent fluxes simulated by the SUEWS model through four MOnitoring LANd Use/Cover Dynamics (MOLAND) scenario runs were evaluated against observations made at two urban and suburban eddy-flux tower sites (i.e., located in a mixed-use area LCZ2 close to Dublin city centre and in a residential green area LCZ6 respectively) in the GDR that are part of the International Urban Flux Network (Keogh et al., 2012). The Dublin Airport station is located approximately 5–10 km distant from the two considered instruments and is located in a warehouse area classified as a large low-rise area (LCZ8), over short grass surfaces, protected behind a Stevenson's screen and away from any building obstructions or similar. The two flux sites are representative of the neighbourhood type in which they are located (Alexander and Mills, 2014) and are assumed to provide observed data within the inertial sublayer (since they are located within almost homogeneous land cover types and at a height which is twice the surrounding roughness elements). The flux data modelled in an imperfect case as in this study i.e., parameters derived by LCZ classification and meteorological data from the Dublin Airport WMO standard station (which is located beyond the urban area) showed good agreement with observations (Alexander et al., 2016; Alexander et al., 2015a, 2015b). Land Surface Temperature (LST) typologies based on land cover and data obtained through MODIS (which provides LST sampled at 1 km resolution) were then generated and the outputs of the SUEWS model were spatially validated (Alexander et al., 2015a, 2015b). This evaluation was conducted over a limited temporal period (April 2010); nevertheless, this period corresponds to a period of cloud-free weather where the model performance is expected to be optimal. Generally, LST was underestimated by SUEWS when compared to observations obtained by MODIS but are consistent with one another.

Fig. 3 provides an overview of the modelling approach employed in this work. As mentioned previously, the SUEWS model requires hourly meteorological data (i.e., of air temperature, precipitation, pressure, wind speed, relative humidity and incoming solar radiation) land cover parameters and estimates of anthropogenic fluxes. In this work, hourly meteorological data for the reference period (baseline) 2000–2015 have been obtained from Dublin Airport WMO standard station to characterize the present mesoscale climate. It is important to note that the SUEWS model does not consider advection which is relevant at the boundary of different surface types. The model assumes a "homogeneous" landscape i.e., the horizontal energy transfer among neighbour cells is considered negligible. Strictly speaking, the model is limited to synoptic conditions associated with strong urban effects i.e., weak airflow, high pressure and clear sky. Sweeney (1987) stated that wind speed is the key factor in mitigating strong UHI development given the geographic location of Dublin city. The Dublin Airport station, being close to the coast, is affected by an afternoon sea-breeze in calm conditions. Indeed, observed temperature measured at the Dublin Airport station are remarkably lower than values observed for the city and the average

Table 1
Outline of the Local Climate Zones (LCZ) present in Dublin city and properties (modified from Alexander et al., 2015a, 2015b; Alexander and Mills, 2014; Stewart and Oke, 2012) in 2010.

LCZ Name and Code	Building surface fraction (%)	Impervious surface fraction (%)	Pervious surface fraction (%)	Height of roughness elements (m)
2 Compact midrise	40–70	30–50	<20	10–25
3 Compact low-rise	40–70	20–50	<30	3–10
5 Open midrise	20–40	30–50	20–40	10–25
6 Open low-rise	20–40	20–50	30–60	3–10
8 Large low-rise	30–50	40–50	<20	3–10
10 Heavy industry	20–40	20–40	40–50	5–15
101 Dense trees	<10	<10	>90	3–30
104 Low plants	<10	<10	>90	<1
105 Bare rock or paved	<10	>90	<10	<0.25
107 Water	<10	<10	>90	–

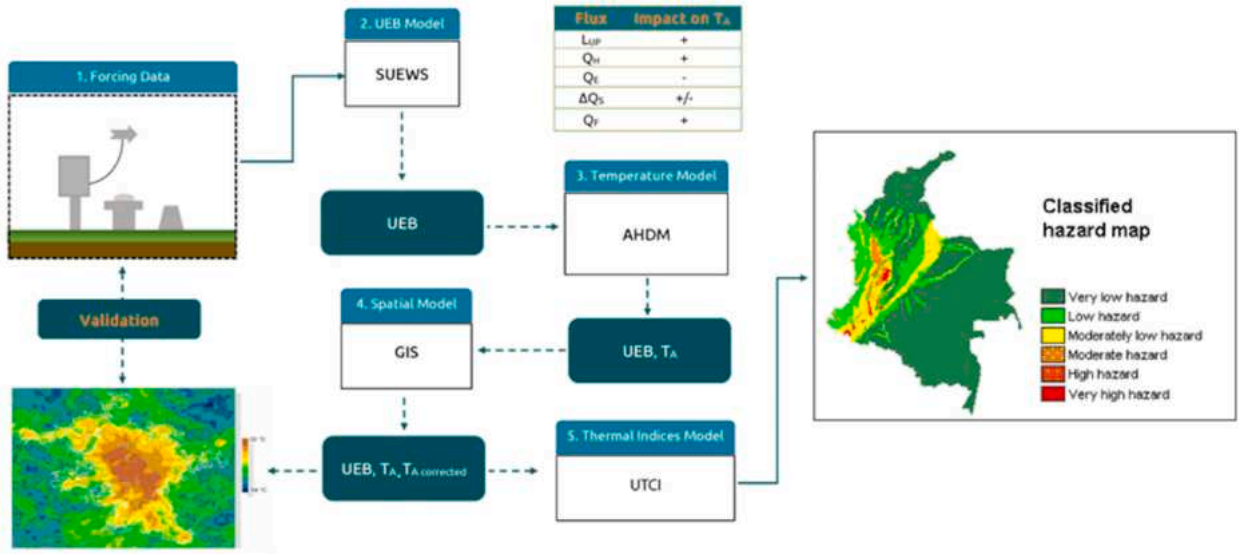

Fig. 3. An overview of the modelling approach employed to integrate the LCZ-based land cover change model and SUEWS to calculate the Hazard index (H) based on UTCI.

wind-speed value at Dublin airport is 2.7 m/s, which is lower than that measured over urban surfaces. As stated in Alexander et al. (2015a, 2015b), such differences are expected for any station located near the area of interest but influenced by its own local climate. Previous empirical work in Dublin (Alexander and Mills, 2014) has shown that within each LCZ "patch", a distinctive thermal characteristic is present and can be readily detected away from the zone boundary. Katabatic winds and sea breezes have not been shown to mute LCZ characteristics. Thus, using data from a WMO standard station such as this, which provides a record of the background climate, to force the SUEWS model, is considered to be a good test of its robustness (Alexander et al., 2015a, 2015b). The SUEWS model obtains humidity, wind and temperature profiles at 30 different levels in the surface layer. In order to account for the canopy layer and roughness sublayer, the SUEWS model follows the Theeuwes et al. (2019) parametrization. It should be noted that these variables are calculated from the forcing data down into the canopy layer, thus assuming that the forcing of humidity and temperature are above the blending height i.e., above which turbulent mixing has levelled out the horizontal gradients of climate variables.

For the purposes of modelling urban-scale changes in climate, future projections of climate have been sourced from Nolan (2015) which provides dynamically downscaled projections for the study area based on two Global Climate Models (GCMs) from the Coupled Model Intercomparison Project Phase 5 (CMIP5; Taylor et al., 2012), namely the UK Met Office's Hadley Centre Global Environment Model version 2 Earth System (HadGEM2-ES) configuration GCM (Collins et al., 2011) and the EC-Earth consortium GCM (Hazeleger et al., 2010). On this basis, Nolan (2015) provides highly resolved modelled climate information for Ireland (at 3 hourly intervals and ranging from 4 to 7 km spatial resolution) employing two RCP scenarios, namely RCP 4.5 and RCP 8.5 (representing medium and high levels of GHG emissions, respectively). RCM output have been validated against observations and confirmed the improved skill over GCMs (Nolan, 2015; Nolan and Flanagan, 2020). The future data of RCM simulations have been obtained at 3 hourly intervals, so a weather generator has been used to obtain hourly values (by means of a statistical downscaling). To derive a Typical Climatological Year (TCY) for the period 2020s (2020–2029), 2030s (2030–2039), 2040s (2040–2049) and 2050s (2050–2059) across both RCPs, values of individual day and month have been averaged across the entire period considered (e.g., average July 2020–2029 = "TCY July" and so forth). Changes in TCY averages are thus reported on an annual basis rather than restricting our analysis to individual events (e.g., heatwaves periods). The choice of the method to create a TCY is mainly related to the limited period of available land cover simulations and climate projections. Indeed, only one normal period would be available. As no corresponding normal would be available for the urban extent based on the current period (1981–2010), it would not be possible to calculate the anomaly from one normal period to the next, except for open grassland LCZ. Secondly, the issue of spatial and temporal scales that are meaningful for policymakers has to be considered. Therefore, a methodology that derives typical conditions for each decade to align urban adaptation targets with the research has been adopted. This kind of approach provides then a benchmark in the study area against which urban planners can fine-tune their adaptation plans to be proactive depending on local circumstances (Bulkeley and Betsill, 2010; Landauer et al., 2018). This dataset has been used to simulate the Urban Energy Budget (UEB) for the region of interest and according to projected changes in land use classes for the period 2020 to 2050. These data are then used as input data for an Analytical Heat Difference Model (AHDM) which relates the components of the UEB model to air temperature. This provides an estimate of air temperature accounting for urban heat (T_a) for Dublin city at a spatial scale of 1 km^2 across the decades 2020s – 2050s and under RCP 4.5 and 8.5. A high resolution DTM (20 m) is used to correct air temperature for the effect of topography (T_a corrected). The lapse rate is based on the spatial correlation between the DTM and observed air temperatures for the period 1981–2010 (Walsh, 2012).

3.1.3. Calculating the universal thermal climate index under climate change

The modelling approach adopted in the previous sections provides a final estimate of T_a corrected. Specifically, these air temperature values account for urban form and urban temperature effects based on a comparison of values for urban sites when compared to the baseline WMO synoptic standard station of Dublin Airport across decades 2020s – 2050s and under RCP 4.5 and 8.5. These corrected values are then used as input to thermal stress models to calculate a hazard indicator. It is important to note that the SUEWS model assumes the absence of radiative transfer within the canyons and that wind and modelled fluxes refer to the inertial sublayer above the canopy, where fluxes are constant with height and microscale variability driven by roughness elements tend to be integrated into local neighbourhood signals (Alexander et al., 2015a, 2015b). This point is relevant because heat stress (Pappenberger et al., 2015) is experienced within the canopy and should thus be considered when analysing the outputs. Nevertheless, few studies measure wind fluxes and speed simultaneously at different heights in and above the Urban Canopy Layer (Theeuwes et al., 2019).

In this work a multi-node model of thermoregulation and human heat transfer has been employed, the Universal Thermal Climate Index (UTCI). The UTCI has been designed and developed by the International Society of Biometeorology (ISB) (Bröde et al., 2012; Jendritzky et al., 2012) and describes how the human body experiences atmospheric conditions leading to heat stress. More specifically, the UTCI is developed conceptually as an equivalent temperature allowing for the interpretation of the index values on a °C unit scale. The reference environment to which all climatic conditions are compared is with 50% relative humidity (vapour pressure not exceeding 2 kPa), calm air and radiant temperature equal to air temperature. Thus, for any combination of air temperature (here T_a corrected), radiation, humidity and wind speed (in the current study, wind speed per day and per hour 10 m above the ground ranges between 0.5 and 30 m/s), UTCI is defined as the air temperature in the reference condition which would cause the same physiological reaction as predicted by the dynamic simulated responses of the physiological model. The UTCI values are further categorized into ten levels of thermal stress from 'extreme cold stress' to 'extreme heat stress' for each month of the climatological year across decades and RCPs. The computation of UTCI through the iterative running of the thermoregulation model is time-consuming. UTCI is operationally estimated based on an established look-up table approach combining regression equations predicting the UTCI and the aforementioned meteorological variables as input (Bröde et al., 2012). Each of the 10 stress levels (Table 2), defined by a specific range of UTCI values, represents the cold/heat stress caused by the physiological and thermoregulatory responses of the human body when reacting to the actual environmental conditions.

In this work, the focus is on the 'extreme heat stress' category (which is assumed as the worst-case scenario) as a proxy of human thermal stress (Table 2), thus results presented afterwards refer to this category only. Moreover, despite UTCI being calculated on an annual basis (i.e., for all months of the TCY), the results presented are for the month of July only, as it is the warmest month based on the 30-years climate normal in Ireland (Met Éireann, 2021).

UTCI values for 'extreme heat stress' category have been mapped and then averaged values for each small area have been obtained. The normalized values (scale from 0 to 1) are calculated using Eq. (1).

$$\beta = \frac{(x - x_{min})}{(x_{max} - x_{min})} \tag{1}$$

where β *is* the normalized value, x the original variable, x_{min} and x_{max} the minimum hazard value (reference period 2020) and maximum hazard value respectively of the dataset (future 2050) over different time periods and RCP scenarios. The normalization procedure allows for the adjustment of values measured at different scale/range and to prevent the generation of spatial biases due to very small/large small areas.

To generate a UTCI-based hazard index including exposure (H from now on), normalized values have been grouped into six categories of increasing hazard (from very low to very high) using equal intervals to show the spatial distributions at the small area level (Fig. 3).

3.2. Heat vulnerability

Vulnerability goes beyond considerations of changes to the climate itself and incorporates the concepts of the sensitivity and adaptive capacity of populations, which can potentially be managed to influence the outcomes of the changes. Sensitivity is the degree to which a system is affected, either adversely or beneficially, by changing climate conditions (IPCC, 2014). Adaptive capacity

Table 2
UTCI categorized in terms of thermal stress (Bröde et al., 2012).

UTCI (°C) range	Stress Category
above +46	extreme heat stress
+38 to +46	very strong heat stress
+32 to +38	strong heat stress
+26 to +32	moderate heat stress
+9 to +26	no thermal stress
+9 to 0	slight cold stress
0 to −13	moderate cold stress
−13 to −27	strong cold stress
−27 to −40	very strong cold stress
below −40	extreme cold stress

addresses the degree to which a system component can adjust to the potential impacts of climate change, the ability to face its consequences and manage adverse conditions or to take advantage of opportunities thus building climate resilience (IPCC, 2014).

The sensitivity and adaptive capacity of an area are dependent on a range of factors including demographic and socio-economic ones (Ellena et al., 2020; Wolf et al., 2013). To assess the sensitivity and adaptive capacity of Dublin city to climate impacts, 2016 national census data have been employed at the small area scale, i.e. the smallest available administrative unit (CSO, 2019b). To determine levels of vulnerability, a range of twelve possible meaningful variables were first considered, based on previous research identifying major factors that have implications for heat-related health impacts and on the availability of CSO dataset. Table 3 outlines the variables and selection rationale considered in this study based on the existing literature.

A statistical-based method which is commonly used for vulnerability assessment i.e. a Principal Component Analysis (PCA), to identify the most important socioeconomic and demographic factors contributing to heat vulnerability was then applied (Alves Menezes et al., 2018; Carter et al., 2016; Hua et al., 2021; Inostroza et al., 2016; Nayak et al., 2018; Paranunzio et al., 2020; Reid et al., 2012, 2009; Rød et al., 2012; Wolf et al., 2013). In summary, PCA maximises the correlation among the original variables to create a set of independent uncorrelated variables or principal components (PCs) that are a linear combination of the original variables (Nardo et al., 2005).

Vulnerability variables are measured using different units, and thus a standardization procedure has been first applied as this standardizes the variables with different ranges and scales using Eq. (2).

$$z = \frac{(x - \mu)}{\sigma} \tag{2}$$

where z *is* the standardized variable, x the original variable, μ the mean and σ the standard deviation. To ensure that high index values indicate high levels of vulnerability in all cases, the index values for indicators hypothesised to decrease risk i.e., the adaptive capacity variables in the vulnerability factor (e.g. information access (households with internet access)) have been reversed. Thus, a new variable "no information access" has been considered instead.

A Pearson correlation matrix has been generated to assess the degree of pair-wise association among the selected variables for vulnerability data. PCA was then used to limit the complexity of the system and reduce the number of variables to fewer components (Cutter et al., 2003; Inostroza et al., 2016; Nayak et al., 2018; Reid et al., 2009; Wolf et al., 2013). A rotation of factors (varimax rotation) was applied to ensure that each variable is maximally correlated with one principal component at a time. Components have been retained based on the following criteria: i) eigenvalues greater than one (Kaiser, 1960), ii) total variance explained above 70%, iii) interpretability criterion based on subjectivity i.e., variables loading on a component should exhibit the same concept and iv) complex-structure variables by loading on multiple factors have been removed. The composite vulnerability index score for each small area is then calculated as the sum of the products of each factor score weighted by the corresponding variance explained by each component. Indeed, a weighted sum using explained variance to weigh each principal component has been used. This kind of approach

Table 3
Variables used to assess vulnerability and the rationale for inclusion.

Variables	Rationale
Urbanization: Population density per km^2	This is a proxy of urban density (Hatvani-Kovacs et al., 2016; Inostroza et al., 2016)
Low income: % population with income below poverty level (unemployed residents having lost job or due to sickness)	The economic status is a proxy of deprivation and could negatively impact on adaptive capacity such as the inability to afford air conditioning, poor general health and life style (Inostroza et al., 2016; Nayak et al., 2018; Paterson and Godsmark, 2020; Wolf et al., 2013)
Housing: % population without house ownership	This is a further proxy of income and deprivation (Hatvani-Kovacs et al., 2016)
Housing: % of old buildings (<1980)	Older homes can also increase vulnerability if they are poorly maintained or insulated, preventing the building from staying at cooler temperatures (Nayak et al., 2018; Stone et al., 2021). Poor-house quality can also be considered a proxy of socioeconomic status and deprivation as well (WHO, 2004).
Social isolation: % population with one-person households	Living alone is a proxy of social isolation. Studies suggest that social isolation can be a key risk factor since many victims of extreme heat are found living alone (Fouillet et al., 2006; Inostroza et al., 2016; Méndez-Lázaro et al., 2018).
Disability: % population with disability	Disabled people (i.e., population with long-term limiting illness or disability) is a proxy of the deterioration of health (Ellena et al., 2020).
Health status: % population with poor health (self-reported health status "not good")	People with poor health are more prone to health impacts and heat-related mortality (Ellena et al., 2020; WHO, 2019)
Extreme ages: % population with age < 15 or > 65 years (extreme ages)	Elderly people and children have been identified as particularly vulnerable groups also in Ireland and more sensitive to adverse heat-related health outcomes, especially during heat wave events in summer (Nayak et al., 2018; Pascal et al., 2013).
Low education: % population with less than a secondary school diploma (low-level education)	Educational level has an influence on how populations respond (Reid et al., 2009).
Travel: % population without a car	The number of people not owning a car is also a proxy of mobility and for access to services (Jiang and O'Neill, 2017).
Information access: % population with internet access	Access to electronic communication and online social networks are factors that influence heat vulnerability (Harlan et al., 2007; Inostroza et al., 2016).
Language isolation: % population with a low level of English	The number of migrants rapidly increased in recent years and emergency alerts in Ireland are issued in English, therefore non-English speakers could miss warnings in weather reports or social media (Nayak et al., 2018).

is based on prior studies on this topic and follows the weighted approach that takes into account the different contribution of each component to explain the spatial pattern of vulnerability to natural hazards (Hua et al., 2021; Schmidtlein et al., 2008; Wolf et al., 2013). In this way, the first PC is given the highest weight and the weights for other PCs decrease accordingly. The final vulnerability index score is normalized to a scale of 0 to 1 and further classified on a six-level scale from very low to very high vulnerability (V) in the same way as for the H index.

3.3. Heat risk

To determine levels of heat-related risk, Hazard (H) and Vulnerability (V) indexes are integrated. In this study, equal weights to account for the influence of each component on the Heat Risk index (HR) via UTCI have been used, thus attributing the same importance to all factors.

$$HR = \frac{1}{2}H + \frac{1}{2}V \tag{3}$$

Again, the HR is further classified on a six-level scale from very low to very high risk in the same way as for the H and V index and finally mapped at small area scale.

4. Results

The level of heat risk has been assessed for all periods and for both RCP 4.5 and 8.5 at the small area scale. Results for the month of July and for extreme heat stress are delineated hereinafter and for the 2020s and 2050s. Results for the intermediate period 2030s and 2040s are included in Section 4.3.

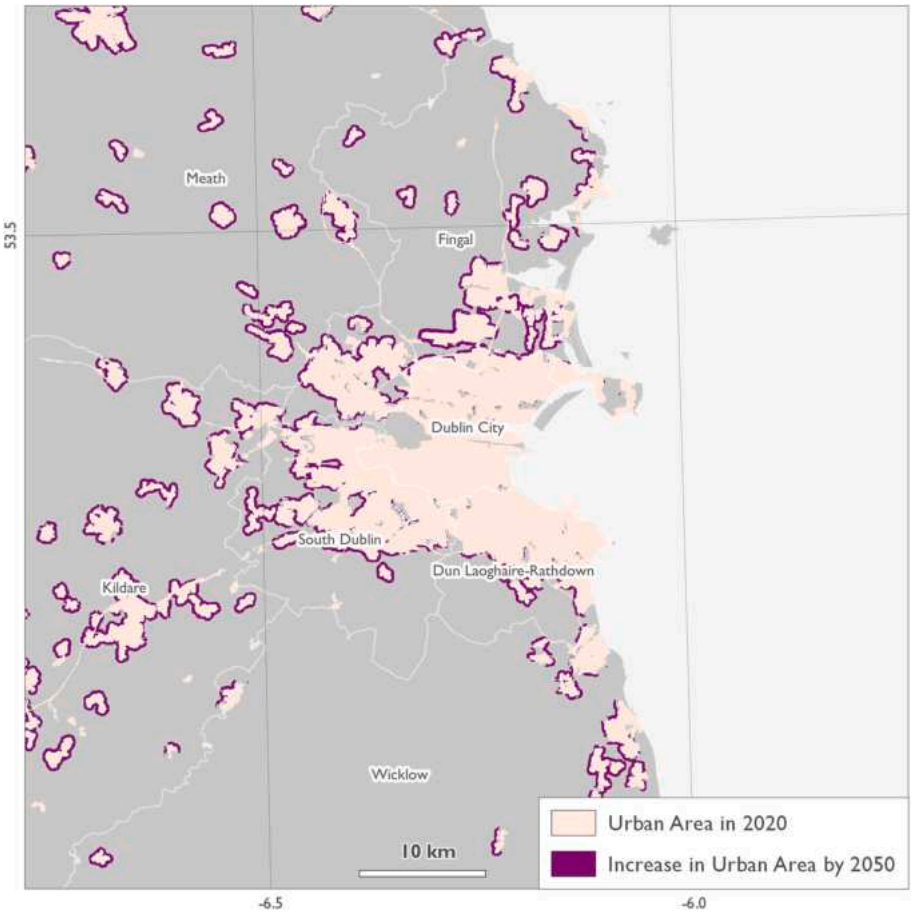

Fig. 4. The modelled increase in urban areas (dense urban, sparse urban, industrial and paved) from 2020 to 2050. The pink area is the urban area in 2020 and the dark purple area shows the increase in urban area from 2020 to 2050. The urban area in 2050 is represented by both the dark purple and pink areas. (For interpretation of the references to colour in this figure legend, the reader is referred to the web version of this article.)

4.1. Projections of exposure and hazard

The enhanced exposure reflected by land cover changes varied and increased gradually across decades (Fig. 4). As highlighted in previous studies (Alexander et al., 2016), compact midrise (LCZ2), open low-rise (LCZ6) and large low-rise (LCZ8) zones collectively capture two thirds of the urban types detected in Dublin City and surrounding areas. Projections indicate that Dublin city centre will remain stable in terms of levels of urbanization, whereas suburban areas will see an increase in urban expansion.

Projected average monthly temperatures (near-surface air temperature, 2 m above ground) have been computed accounting for the UHI effect (T_a corrected) on a decadal basis for the period 2020s–2050s under both RCP 8.5 and 4.5 scenarios. Fig. 5 shows T_a corrected for July in the 2020s and 2050s under both scenarios. Fig. 6 shows the differences between T_a calculated for the 2020s and 2050s under both RCP scenarios. Warming is greatest in the Greater Dublin Area (GDA) (which is most pronounced for the urban centre as a result of the UHI effect). Under the RCP 8.5 scenario, exposure to high temperatures is expected to increase considerably and be pervasive across the entire study area with values ranging between 10.5 and 17.5 °C in the non-urban classes. In the urban classes, an increase in minimum values is seen with values greater than 14.5 °C, while the maximum value is still around 17.5 °C. In areas converted from non-urban to urban, the temperature range is similar to the latter, between 14 and 17.5 °C. Thus under the worst-case scenario RCP8.5, the increase in mean temperature values in the converted areas in 2050s with respect to the 2020s is 0.95 °C (Fig. 6), while for areas those areas which remain urban the increase is smaller (0.88 °C) (Fig. 6). Under RCP4.5, the increase in mean temperatures between 2020s and 2050s is limited to 0.3 °C for areas converted from non-urban to urban and to 0.23 °C for those areas which remain urban.

Fig. 7 shows the exposure to strong heat stress hazard (H) in terms of UTCI for the month of July at the small area scale across

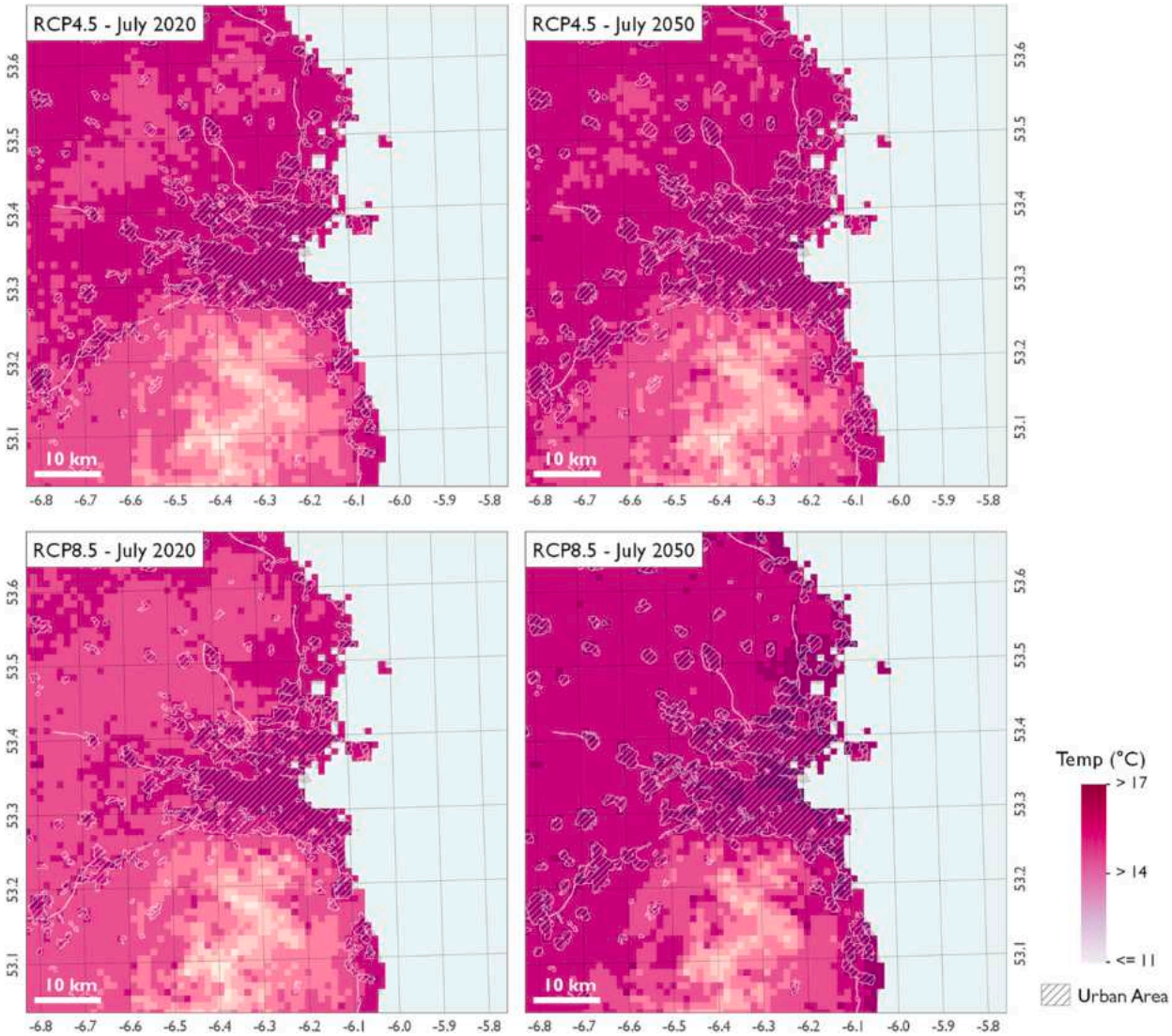

Fig. 5. Corrected monthly average air temperature (T_a) for the 2020s and 2050s under RCP 4.5 and 8.5 in the month of July.

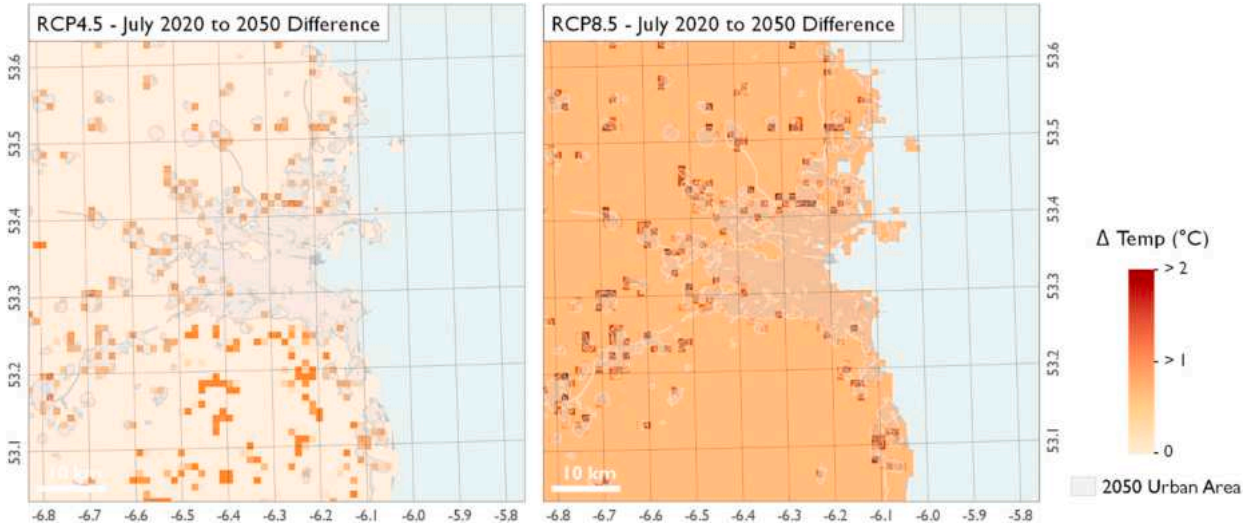

Fig. 6. The modelled differences between 2020 and 2050 in corrected monthly average air temperature (T_a) under RCP 4.5 and 8.5 in the month of July.

periods and RCPs. Comparing maps of land cover changes, mean air temperature and hazard, it is evident that the impact caused by RCP scenario and temperature increase is greater when compared to the impact of urban expansion, particularly in the core city centre. Note that under both scenarios there is an increase in the number of hours of exposure across the region in the 2050s compared to the 2020s. Small areas included in the higher ranking (from 4 to 6) increase by 83% and 28% under RCP 4.5 and 8.5 respectively. This is indicative of the fact that in a hypothetical worst-case RCP scenario the level of heat stress in Dublin city during the period 2021–2029 would be similar to the one detected in the 2050s under an intermediate scenario RCP 4.5. The increase in the number of small areas included in the higher ranking in the 2050s under RCP 8.5 is 44% when compared to the same period under RCP 4.5. In the RCP 8.5 scenario, the combined effect of the urban footprint and climate change in 2050s is particularly evident across the entire city and suburbs with the exception of green/blue areas (e.g., Phoenix Park, Fig. 7, 53.36, −6.33). Focussing on the peripheries, the north-eastern part of the city up to the airport area and the western end of the city (Fig. 7, Cherry Orchard, −53.33°, −6.36°, Drumfinn, −53.34°, −6.36°, Kylemore, −53.33°, −6.35°) are included in the highest heat stress level in 2050s.

4.2. Current vulnerability

Of the 13 variables selected, 7 variables were omitted during the PCA process as they loaded on more than one component. The reason behind this is related to the fact that when a variable is factorially complex (that is, it loads on several components) problems of interpretation are aggravated. On this basis, six components were extracted but only the first two are considered significant following the Kaiser rule. Table 4 presents correlations among the final six variables selected for this analysis.

Most of the data structure was captured in the first two components which account for 72.2% of the total variance in the data. Others PCs do not fulfil Kaiser's rule and therefore, they are not considered for further analysis. The first component has an eigenvalue of 3.03, explaining 50.5% of the variance. The second PC has an eigenvalue of 1.3, accounting for 21.7% of the total variance. Table 5 shows the results of the PCA for the current period. The dominating variables in PC1 include the following: "low income", "low education", "disability" and "no information access" variables, while "social isolation" and "extreme ages" are relevant for PC2.

Fig. 8 displays the spatial distribution of the Vulnerability index for the current period (based on 2016) across small areas in Dublin city. Within Dublin city itself there are numerous adjacent areas of lower and higher vulnerability and with an outer ring of higher vulnerability values towards the west and north of the city. This is in line with the Pobal HP Deprivation Index which measures the relative disadvantage or affluence of all small areas around Ireland based on socioeconomic variables (Pobal, 2019). This highlights the importance of deprivation in determining levels of social vulnerability under prevailing socio-economic conditions. The correspondence between this vulnerability index and deprivation studies could pose the basis to use this in future assessments to link with the social science community.

The more disadvantaged areas are those in Ballyfermot in the western end of the city, part of Priorswood, Ballymun and Finglas in the north-north-western part of the city and some small areas around and in the core city centre (e.g. part of North Dock, Cabra, Merchants Quay, Usher). These areas are generally characterized by relatively high percentages of age dependency, lone parent ratios and socially isolated people, along with persons with disabilities and high unemployment rate. However, based on the six-scale categorization adopted, the current vulnerability is relatively low in most parts of the study area, since the majority of the small areas (more than 82%) are considered to be of lower vulnerability (levels 1 to 3). Low levels of vulnerability are seen, besides the parks, in the most affluent areas i.e., the core city centre and the whole southern part of the city. In these areas, although moderately high levels of heat stress are seen, levels of vulnerability are reduced due to residents having a high standard of living and socioeconomic

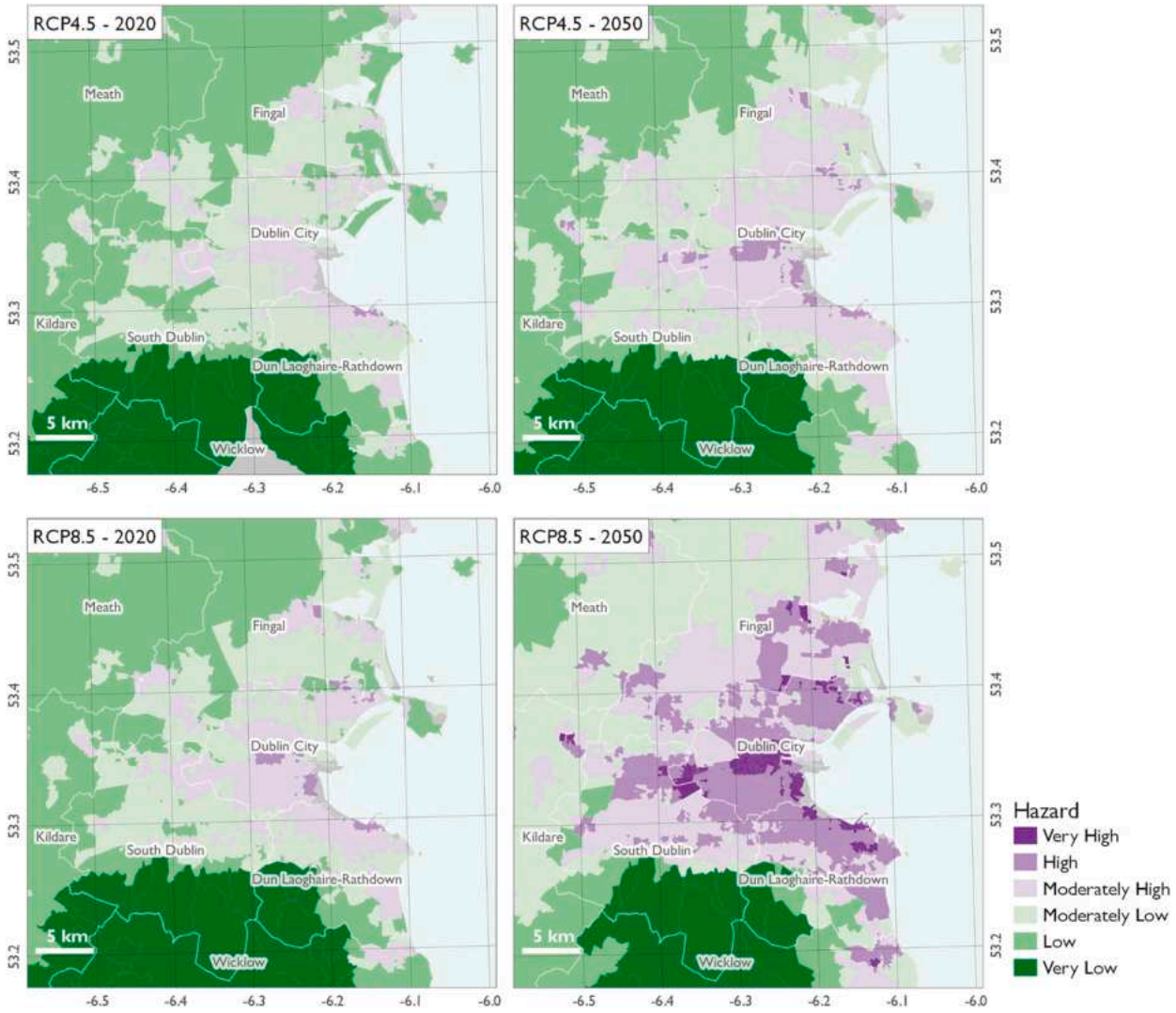

Fig. 7. UTCI-based Hazard (H) index under RCP 4.5 and 8.5 for the 2020s and 2050s in the month of July. In this work, in terms of UTCI, the focus is on the 'extreme heat stress' category only. The final hazard indicator has been classified from very low to very high hazard.

Table 4
Pearson's correlation coefficient for final selected sensitivity and adaptive capacity variables in Dublin city. Values with asterisk show non-significant correlation with *p*-values >0.05.

Variables	Low income	Social isolation	Low education	Disability	Extreme ages	No information access
Low income	1.00	0.23	0.65	0.53	0.02*	0.56
Social isolation		1.00	0.11	0.40	−0.19	0.54
Low education			1.00	0.62	0.35	0.66
Disability				1.00	0.30	0.52
Extreme ages					1.00	0.11
No information access						1.00

status.

4.3. Heat risk projections

In this section, as for H mapping, results for the Heat Risk index (HR) for the 2020s and the 2050s under both RCP 4.5 and 8.5 are presented (Fig. 9). Values for H, V and HR related to the intermediate periods 2030s–2040s are provided in Table 6.

In the 2050s (Fig. 9), the HR appears to increase in the suburbs of regional towns for both RCPs with respect to the 2020s baseline

Table 5
Eigenvalues and outputs from Principal Component Analysis for the Vulnerability. Variables Rotated factor pattern: varimax rotation method. Significant values are marked with an asterisk.

Variables	PC1	PC2
Low income	0.44*	−0.07
Social isolation	0.24	−0.63*
Low education	0.50*	0.24
Disability	0.47*	0.05
Extreme ages	0.20	0.70*
No information access	0.47*	−0.22
Variance explained	**50.5%**	**21.7%**
Eigenvalues	**3.03**	**1.3**

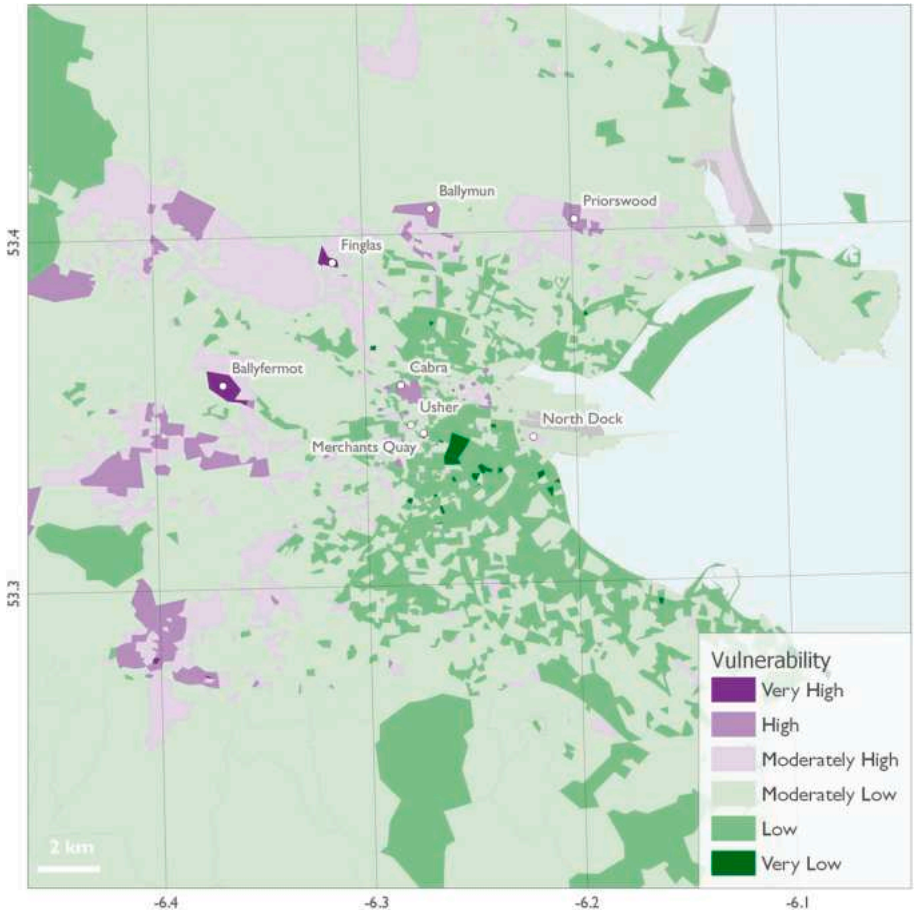

Fig. 8. Vulnerability (V) index for the current period based on the weightings in PC1 and PC2 for the current period in Dublin city.

and as a result of the urban effect. Nonetheless, the increase under RCP 4.5 is visibly less pronounced than the one expected under the worst-case RCP 8.5 scenario. Under RCP 4.5 and 8.5, the number of areas particularly vulnerable to heat (levels 4–6) will increase by 70% and 96% respectively between the 2020s and the 2050s. Small areas falling in the highest ranking in 2050s are projected to increase by 44% under RCP 8.5 with respect to the moderate RCP 4.5. The mean value of HR across the entire study area under RCP 8.5 increases from 3.3 to 4 between the 2020s and the 2050s, whereas the shift is more limited under RCP 4.5 (from 3.1 to 3.4). The gradual decrease/increase in the percentage of small areas included in the lowest levels (1 to 3)/highest levels (4 to 6) is also visible in the intermediate periods of the 2030s and the 2040s respectively (Table 6).

In the current period, the core city centre and the northern and south-western peripheries are the areas where the highest heat risk is seen. The city centre is surrounded by an outer ring of moderately low risk areas under both RCPs, except for a north-western artery linking the core city to Cabra and Ashtown (Fig. 9, 53.37°, −6.32°). In the future under RCP 4.5, the trend looks similar with an intensification of heat risk level in the areas which were already in the highest levels. Under RCP 8.5, almost the entire study area will

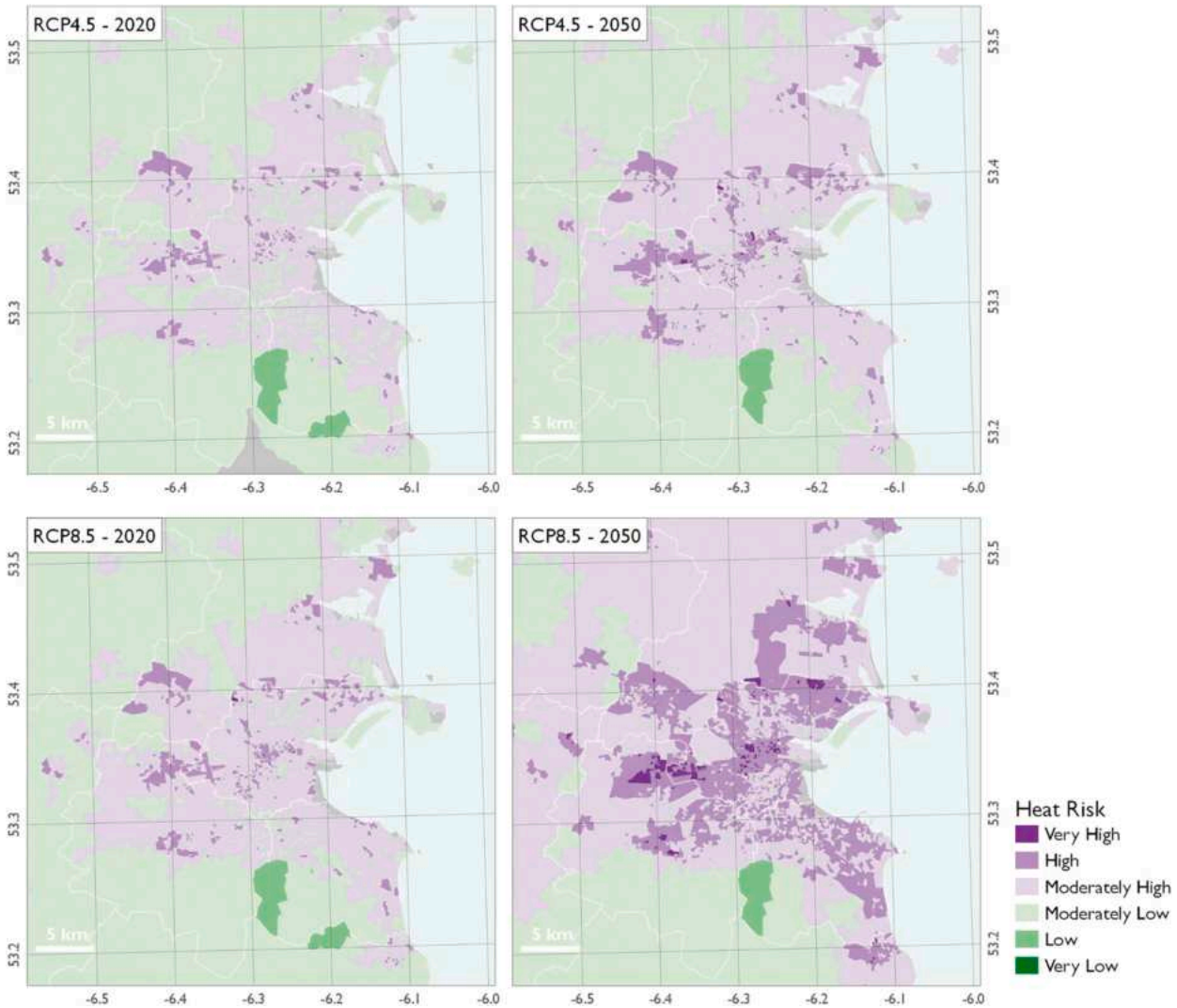

Fig. 9. Heat Risk index across Dublin city under a RCP 4.5 and 8.5 for the 2020s and 2050s during the month of July.

Table 6
Percentage of small areas included in each level 1 to 6 (1 = very low, 2 = low, 3 = moderately low, 4 = moderately high, 5 = high, 6 = very high) of Hazard (H), Vulnerability (V) and Heat Risk index (HR) levels across 2020s, 2030s, 2040s and 2050s under RCP 4.5 and 8.5.

	2020s			2030s			2040s			2050s		
	H	V	R	H	V	R	H	V	R	H	V	R
RCP 4.5												
1	0.0	1.0	0.0	0.0	1.0	0.0	0.0	1.0	0.0	0.0	1.0	0.0
2	3.2	34.8	1.2	1.6	34.8	0.9	1.4	34.8	0.7	0.1	34.8	0.1
3	48.7	46.7	60.3	40.2	46.7	55.6	36.4	46.7	53.4	11.8	46.7	34.4
4	48.1	15.0	37.1	56.6	15.0	41.8	60.5	15.0	44.2	68.4	15.0	59.6
5	0.0	2.4	1.4	1.6	2.4	1.7	1.7	2.4	1.7	19.7	2.4	5.8
6	0.0	0.1	0.0	0.0	0.1	0.0	0.0	0.1	0.0	0.0	0.1	0.0
RCP 8.5												
1	0.0	1.0	0.0	0.0	1.0	0.0	0.0	1.0	0.0	0.0	1.0	0.0
2	2.3	34.8	3.2	1.9	34.8	1.2	0.0	34.8	0.0	0.0	34.8	0.0
3	20.9	46.7	48.7	55.8	46.7	62.6	3.4	46.7	14.7	1.6	46.7	5.7
4	68.9	15.0	48.1	42.2	15.0	34.7	36.5	15.0	70.5	13.3	15.0	69.3
5	7.9	2.4	0.0	0.0	2.4	1.5	52.0	2.4	14.7	60.8	2.4	24.1
6	0.0	0.1	0.0	0.0	0.1	0.0	8.1	0.1	0.1	24.3	0.1	0.9

be included in the moderate to very high levels of risk with very few exceptions, those being mainly around the Clontarf area (Fig. 9, −53.36°, −6.18°).

5. Discussion

As climate change progresses, risk assessments are becoming increasingly important in planning to offset adverse climate change impacts. This is particularly the case for urban areas which are considered to be particularly at risk. This study employs the IPCC AR5 definition of risk to determine spatial and temporal variations in levels of strong heat stress (hazard) for the Dublin area and accounts for exposure of the region and vulnerability of the population.

Accounting for projected temperature change, the UHI effect and projected changes in urban development, results indicate that replacement of natural landscapes with artificial material, particularly in the peri-urban areas of the Dublin region would inevitably impact upon the surface energy budget. Moreover, most parts of these areas are identified as zones for further high-density development, potentially leading to a reduction in green areas available, thus accentuating the UHI effect with possible health and well-being implications for the population (Gronlund et al., 2015).

For Dublin city projected air temperature increases on a regional basis are being amplified by the UHI effect as highlighted in recent studies in other high-density cities (Hua et al., 2021; Verdonck et al., 2019). Accounting for the amplification of future regional temperature increases in urban centres as a result of UHI is becoming increasingly important for the development of city specific mitigation and adaptation policies as the non-stationary nature of UHI over time complicates such studies (Schatz and Kucharik, 2015).

In determining exposure, this study recognises the limitation of the methodology employed and particularly in terms of future projections of changes in the biophysical components of risk. This work accounts for a proportion of the uncertainty inherent in projected future climate by looking at outcomes under two IPCC scenarios: one based on medium (RCP 4.5) and the other on high emissions (RCP 8.5). Irrespective of scenario, the study demonstrates that the exposure of Dublin city to heat hazard is projected to increase considerably from the 2020s to the 2050s, with the impacts and potential risk being more accentuated under the worst-case emissions scenario. In assessing the effects of UHI on regional projections of climate change, it is recognised that there is an inherent assumption that UHI intensity is stable and comparable to the reference period. Moreover, the modelling approach employed derive changes in air temperature for the future period only and not for changes in air circulation which has been shown to influence background weather conditions that generate heatwaves and UHI.

In the coming decades, the risks posed by climate change will not only be driven by physical impacts but will also be dependent on the vulnerability of the exposed populations and infrastructure. In this study, spatial socio-economic data from national census data (CSO, 2019b) has been used to estimate the vulnerability of populations in small areas across Dublin city.

To explore the vulnerability component related to heat risk, a methodology based on PCA has been used. This approach captures all relevant aspects of the vulnerability of the study area, but some limitations still remain. For example, the authors are aware of the fact that the considered variables do not explain patterns of heat vulnerability equally. Nevertheless, a priori assumption of their relative importance in terms of effects and contributions on heat vulnerability could introduce biases in the final assessment and PCA is a standard and widely used procedure in vulnerability assessment and mapping to reduce and remove redundant variables to allow easier understanding and interpretation of the phenomena (Carter et al., 2016; Inostroza et al., 2016; Nayak et al., 2018; Reid et al., 2009; Wolf et al., 2013). In this study, vulnerability has not been projected in the future and this represents a limitation in the framework of risk studies. Data from the 2016 census were employed to assess vulnerability across current and future periods. As such, it does not incorporate potential changes in population and socio-economics or the changing age profile. This means that vulnerability has been assessed only for the current period and is assumed to remain the same in the future i.e., it is stationary across decades. As a result, it is likely that heat risk for future periods is underestimated. Nonetheless, this methodology is in line with other recent state of the art international studies, where future socio-economic projections are not included (de Sherbinin et al., 2019). The outcomes presented could therefore be considered the best-case scenario, as it is projected that the population will increase across Dublin city and that average age will increase. These changes will all lead to exacerbated levels of vulnerability and risk unless actions are taken to address areas of sensitivity or enhance adaptive capacity. In this framework, shared socio-economic pathways are an emerging approach which will allow better incorporation of future socio-economic conditions.

This work identifies that the climate change risk is not merely a result of different exposures to climate-related hazards but a result of social and economic factors. The indexes developed in this work are a valuable tool to inform urban planning and management decisions and can be used to conduct participatory and open public discussion. Adaptation and mitigation measures should thus be focused on those areas in need of the more urgent interventions i.e., characterized by high risk due to higher hazard and exposure and/or higher levels of vulnerability. Moreover, this work provides a multi-disciplinary view on vulnerability and highlights that the level of risk posed by climate change hazards on populations is determined by factors such as income, housing, health, demographics and social connectedness. As such the indicators provides a valuable tool to identify further areas of research into the factors that contribute to vulnerability.

The proposed methodology provides a step-by-step approach for developing indicators that illustrate each of the three core components of risk at spatial scales that can be understood by urban planners and prompt consideration of important topics. By illustrating the components of risk, the methodology provides insights into how the planning system can contribute to the reduction of climate risks. Moreover, a broad range of factors have been included and these are likely to apply to a range of climate hazards.

6. Conclusions

This work has provided spatially explicit information on the evolution of climate change risk for Dublin city in relation to heat over the coming decades. A highly innovative aspect of this work is that it makes use of an integrated approach which allows for the urban heat effect to be accounted for and to derive an improved thermal heat stress index (i.e., UTCI) as a hazard indicator. Moreover, it uses spatially disaggregated socio-economic data to calculate the sensitivity and adaptive capacity of communities across Dublin city at the finest available spatial scale. Tailored indices are thus calculated and mapped to highlight the level of risk to extreme heat stress hazard in terms of UTCI both spatially and temporally under projected climate change. Such information has the potential to support planners in prioritising areas and communities for the development and implementation of climate adaptation measures and to increase resilience to climate change impacts at local scale.

Declaration of Competing Interest

The authors declare that they have no known competing financial interests or personal relationships that could have appeared to influence the work reported in this paper.

Acknowledgements

The authors acknowledge the financial support of the Large Urban Area Adaptation (Urb-ADAPT) project (2015-CCRP-MS.25) in the EPA Research Programme 2014–2020, which is a Government of Ireland initiative funded by the Department of Communications, Climate Action and Environment, administered by the Environmental Protection Agency. The authors would like to acknowledge the members of the Project Steering Committee and the support of the Project Manager on behalf of EPA Research. The authors would like to gratefully thank our project partner, the Eastern and Midlands Regional Assembly, particularly the contribution of Travis O'Doherty. The insights of those who attended workshops and conference presentations were also invaluable for this study.

References

Alexander, P.J., Mills, G., 2014. Local climate classification and Dublin's urban heat island. Atmosphere (Basel). 5, 755–774. https://doi.org/10.3390/atmos5040755.
Alexander, P.J., Fealy, R., Mills, G., 2015a. Spatial validation of an urban energy balance model using multi-temporal remotely sensed surface temperature. 2015 Jt. Urban Remote Sens. Event. https://doi.org/10.1109/JURSE.2015.7120500. JURSE 2015.
Alexander, P.J., Mills, G., Fealy, R., 2015b. Using LCZ data to run an urban energy balance model. Urban Clim. 13, 14–37. https://doi.org/10.1016/j.uclim.2015.05.001.
Alexander, P.J., Fealy, R., Mills, G.M., 2016. Simulating the impact of urban development pathways on the local climate: a scenario-based analysis in the greater Dublin region, Ireland. Landsc. Urban Plan. 152, 72–89. https://doi.org/10.1016/J.LANDURBPLAN.2016.02.006.
Alexander, P.J., O'Dwyer, B., Brennan, M., Mills, G., Lynch, P., 2017. Land surface temperature climatology over urban surfaces: A blended approach. 2017 Jt. Urban Remote Sens. Event. https://doi.org/10.1109/JURSE.2017.7924599. JURSE 2017.
Alves Menezes, J., Confalonieri, U., Paula Madureira, A., de Brito Duval, I., Barbosa dos Santos, R., Margonari, C., 2018. Mapping Human Vulnerability to Climate Change in the Brazilian. The construction of a municipal vulnerability index, Amazon. https://doi.org/10.1371/journal.pone.0190808.
Arnfield, A.J., 2003. Two decades of urban climate research: A review of turbulence, exchanges of energy and water, and the urban heat island. Int. J. Climatol. 23, 1–26. https://doi.org/10.1002/joc.859.
Barnett, A., Tong, S., Clements, A., 2009. Abstracts of the international society for environmental epidemiology 21st annual conference. August 25–29, 2009. Dublin, Ireland. Epidemiology 20, 13–265.
Barriopedro, D., Fischer, E.M., Luterbacher, J., Trigo, R.M., García-Herrera, R., 2011. The hot summer of 2010: redrawing the temperature record map of Europe. Science (80-.). 332, 220–224. https://doi.org/10.1126/science.1201224.
Bechtel, B., Alexander, P.J., Böhner, J., Ching, J., Conrad, O., Feddema, J., Mills, G., See, L., Stewart, I., 2015. Mapping local climate zones for a worldwide database of the form and function of cities. ISPRS Int. J. Geo-Inform. 4, 199–219. https://doi.org/10.3390/ijgi4010199.
Bröde, P., Fiala, D., Blazejczyk, K., Holmér, I., Jendritzky, G., Kampmann, B., Tinz, B., Havenith, G., 2012. Deriving the operational procedure for the universal thermal climate index (UTCI). Int. J. Biometeorol. 56, 481–494. https://doi.org/10.1007/s00484-011-0454-1.
Bulkeley, H., Betsill, M., 2010. Rethinking Sustainable Cities: Multilevel Governance and the "Urban" Politics of Climate Change, 14, pp. 42–63. https://doi.org/10.1080/0964401042000310178.
Cámaro García, Walther C.A., Dwyer, Ned, 2021. Climate Status Report for Ireland 2020. Environmental Protection Agency, Wexford, Ireland.
Carter, T.R., Fronzek, S., Inkinen, A., Lahtinen, I., Lahtinen, M., Mela, H., Brien, K.L.O., Rosentrater, L.D., Ruuhela, R., Simonsson, L., Terama, E., O'Brien, K.L., Rosentrater, L.D., Ruuhela, R., Simonsson, L., Terama, E., 2016. Characterising vulnerability of the elderly to climate change in the Nordic region. Reg. Environ. Chang. 16, 43–58. https://doi.org/10.1007/s10113-014-0688-7.
Chakraborty, T., Hsu, A., Manya, D., Sheriff, G., 2020. A spatially explicit surface urban heat island database for the United States: characterization, uncertainties, and possible applications. ISPRS J. Photogramm. Remote Sens. 168, 74–88. https://doi.org/10.1016/j.isprsjprs.2020.07.021.
Chapman, S., Watson, J.E.M.M., Salazar, A., Thatcher, M., McAlpine, C.A., 2017. The impact of urbanization and climate change on urban temperatures: a systematic review. Landsc. Ecol. 32, 1921–1935. https://doi.org/10.1007/s10980-017-0561-4.
Chow, W.T.L., Chuang, W.C., Gober, P., 2012. Vulnerability to extreme heat in metropolitan phoenix: spatial, temporal, and demographic dimensions. Prof. Geogr. 64, 286–302. https://doi.org/10.1080/00330124.2011.600225.
Collins, W.J., Bellouin, N., Doutriaux-Boucher, M., Gedney, N., Halloran, P., Hinton, T., Hughes, J., Jones, C.D., Joshi, M., Liddicoat, S., Martin, G., O'Connor, F., Rae, J., Senior, C., Sitch, S., Totterdell, I., Wiltshire, A., Woodward, S., 2011. Development and evaluation of an earth-system model - HadGEM2. Geosci. Model Dev. 4, 1051–1075. https://doi.org/10.5194/gmd-4-1051-2011.
Copernicus Land Monitoring Service, 2021. CORINE Land Cover — Copernicus Land Monitoring Service [WWW Document]. URL. https://land.copernicus.eu/pan-european/corine-land-cover (accessed 3.29.21).
CSO, 2019a. Census 2016 Profile 3 - an Age Profile of Ireland - CSO - Central Statistics Office [WWW Document]. URL. https://www.cso.ie/en/csolatestnews/presspages/2017/census2016profile3-anageprofileofireland/.
CSO, 2019b. Census 2016 Small Area Population Statistics - CSO - Central Statistics Office [WWW Document]. URL. https://www.cso.ie/en/census/census2016reports/census2016smallareapopulationstatistics/ (accessed 1.7.19).
Cutter, S.L., Boruff, B.J., Shirley, W.L., 2003. Social vulnerability to environmental hazards *. Soc. Sci. Q. 84, 242–261. https://doi.org/10.1111/1540-6237.8402002.

de Sherbinin, A., Bukvic, A., Rohat, G., Gall, M., McCusker, B., Preston, B., Apotsos, A., Fish, C., Kienberger, S., Muhonda, P., Wilhelmi, O., Macharia, D., Shubert, W., Sliuzas, R., Tomaszewski, B., Zhang, S., 2019. Climate vulnerability mapping: A systematic review and future prospects. Wiley Interdiscip. Rev. Clim. Chang. 10, 1–23. https://doi.org/10.1002/wcc.600.

Di Napoli, C., Pappenberger, F., Cloke, H.L., 2018. Assessing heat-related health risk in Europe via the universal thermal climate index (UTCI). Int. J. Biometeorol. 62, 1155–1165. https://doi.org/10.1007/s00484-018-1518-2.

Éireann, Met, 2021. Monthly Data - Met Éireann - the Irish Meteorological Service [WWW Document]. URL. https://www.met.ie/climate/available-data/monthly-data.

Ellena, M., Breil, M., Soriani, S., 2020. The heat-health nexus in the urban context: A systematic literature review exploring the socio-economic vulnerabilities and built environment characteristics. Urban Clim. 34, 100676. https://doi.org/10.1016/j.uclim.2020.100676.

Estoque, R.C., Ooba, M., Seposo, X.T., Togawa, T., Hijioka, Y., Takahashi, K., Nakamura, S., 2020. Heat health risk assessment in Philippine cities using remotely sensed data and social-ecological indicators. Nat. Commun. 11, 1–12. https://doi.org/10.1038/s41467-020-15218-8.

European Environment Agency, 2019. The European Environment — State and Outlook 2020 — European Environment Agency [WWW Document]. URL. https://www.eea.europa.eu/publications/soer-2020.

Fouillet, A., Rey, G., Laurent, F., Pavillon, G., Bellec, S., Guihenneuc-Jouyaux, C., Clavel, J., Jougla, E., Hémon, D., 2006. Excess mortality related to the August 2003 heat wave in France. Int. Arch. Occup. Environ. Health 80, 16–24. https://doi.org/10.1007/s00420-006-0089-4.

Gasparrini, A., Guo, Y.L.Y., Sera, F., Vicedo-Cabrera, A.M., Huber, V., Tong, S., de Sousa Zanotti Stagliorio Coelho, M., Nascimento Saldiva, P.H., Lavigne, E., Matus Correa, P., Valdes Ortega, N., Kan, H., Osorio, S., Kyselý, J., Urban, A., Jaakkola, J.J.K., Ryti, N.R.I., Pascal, M., Goodman, P.G., Zeka, A., Michelozzi, P., Scortichini, M., Hashizume, M., Honda, Y., Hurtado-Diaz, M., Cesar Cruz, J., Seposo, X., Kim, H., Tobias, A., Iñiguez, C., Forsberg, B., Åström, D.O., Ragettli, M.S., Guo, Y.L.Y., Wu, C., Zanobetti, A., Schwartz, J., Bell, M.L., Dang, T.N., Do Van, D., Heaviside, C., Vardoulakis, S., Hajat, S., Haines, A., Armstrong, B., 2017. Projections of temperature-related excess mortality under climate change scenarios. Lancet Planet. Heal. 1, e360–e367. https://doi.org/10.1016/S2542-5196(17)30156-0.

Georgiadis, T., 2017. Urban Climate and Risk, pp. 1–29. https://doi.org/10.1093/oxfordhb/9780190699420.013.11.

Gronlund, C.J., Berrocal, V.J., White-Newsome, J.L., Conlon, K.C., O'Neill, M.S., 2015. Vulnerability to extreme heat by socio-demographic characteristics and area green space among the elderly in Michigan, 1990-2007. Environ. Res. 136, 449–461. https://doi.org/10.1016/j.envres.2014.08.042.

Guerreiro, S.B., Dawson, R.J., Kilsby, C., Lewis, E., Ford, A., Guerreiro, S.B., Ford, A., Dawson, R.J., Kilsby, C., Lewis, E., Ford, A., Guerreiro, S.B., Ford, A., Dawson, R. J., Kilsby, C., 2018. Future heat-waves, droughts and floods in 571 European cities. Environ. Res. Lett. 13, 034009 https://doi.org/10.1088/1748-9326/aaaad3.

Guo, Y., Gasparrini, A., Armstrong, B.G., Tawatsupa, B., Tobias, A., Lavigne, E., De Sousa Zanotti Stagliorio Coelho, M., Pan, X., Kim, H., Hashizume, M., Honda, Y., Leon Guo, Y.L., Wu, C.F., Zanobetti, A., Schwartz, J.D., Bell, M.L., Scortichini, M., Michelozzi, P., Punnasiri, K., Li, S., Tian, L., Garcia, S.D.O., Seposo, X., Overcenco, A., Zeka, A., Goodman, P., Dang, T.N., Van Dung, D., Mayvaneh, F., Saldiva, P.H.N., Williams, G., Tong, S., 2017. Heat wave and mortality: a multicountry, multicommunity study. Environ. Health Perspect. 125, 1–11. https://doi.org/10.1289/EHP1026.

Harlan, S.L., Brazel, A.J., Darrel Jenerette, G., Jones, N.S., Larsen, L., Prashad, L., Stefanov, W.L., 2007. In the shade of affluence: the inequitable distribution of the urban heat island. Res. Soc. Probl. Public Policy. https://doi.org/10.1016/S0196-1152(07)15005-5.

Hatvani-Kovacs, G., Belusko, M., Skinner, N., Pockett, J., Boland, J., 2016. Heat stress risk and resilience in the urban environment. Sustain. Cities Soc. 26, 278–288. https://doi.org/10.1016/j.scs.2016.06.019.

Hazeleger, W., Severijns, C., Semmler, T., Ştefănescu, S., Yang, S., Wang, X., Wyser, K., Dutra, E., Baldasano, J.M., Bintanja, R., Bougeault, P., Caballero, R., Ekman, A. M.L., Christensen, J.H., Van Den Hurk, B., Jimenez, P., Jones, C., Kållberg, P., Koenigk, T., McGrath, R., Miranda, P., Van Noije, T., Palmer, T., Parodi, J.A., Schmith, T., Selten, F., Storelvmo, T., Sterl, A., Tapamo, H., Vancoppenolle, M., Viterbo, P., Willén, U., 2010. EC-earth: a seamless earth-system prediction approach in action. Bull. Am. Meteorol. Soc. 91, 1357–1363. https://doi.org/10.1175/2010BAMS2877.1.

Hua, J., Zhang, X., Ren, C., Shi, Y., Lee, T.C., 2021. Spatiotemporal assessment of extreme heat risk for high-density cities: a case study of Hong Kong from 2006 to 2016. Sustain. Cities Soc. 64 https://doi.org/10.1016/j.scs.2020.102507.

Imhoff, M.L., Zhang, P., Wolfe, R.E., Bounoua, L., 2010. Remote sensing of the urban heat island effect across biomes in the continental USA. Remote Sens. Environ. 114, 504–513. https://doi.org/10.1016/j.rse.2009.10.008.

Inostroza, L., Palme, M., De La Barrera, F., 2016. A heat vulnerability index: spatial patterns of exposure, sensitivity and adaptive capacity for Santiago de Chile. PLoS One 11, 1–26. https://doi.org/10.1371/journal.pone.0162464.

IPCC, 2014. Climate Change 2014: Impacts, Adaptation and Vulnerability - Contributions of the Working Group II to the Fifth Assessment Report. [WWW Document]. Clim. Chang. 2014 Impacts, Adapt. Vulnerability - Contrib. Work. Gr. II to Fifth Assess. Rep. URL. http://www.ipcc.ch/pdf/assessment-report/ar5/wg2/ar5_wgII_spm_en.pdf.

Järvi, L., Grimmond, C.S.B., Christen, A., 2011. The surface urban energy and water balance scheme (SUEWS): evaluation in Los Angeles and Vancouver. J. Hydrol. 411, 219–237. https://doi.org/10.1016/j.jhydrol.2011.10.001.

Jendritzky, G., de Dear, R., Havenith, G., 2012. UTCI—why another thermal index? Int. J. Biometeorol. 56, 421–428. https://doi.org/10.1007/s00484-011-0513-7.

Jiang, L., O'Neill, B.C., 2017. Global urbanization projections for the shared socioeconomic pathways. Glob. Environ. Chang. 42, 193–199. https://doi.org/10.1016/J.GLOENVCHA.2015.03.008.

Kaiser, H.F., 1960. The application of electronic computers to factor analysis. Educ. Psychol. Meas. 20, 141–151. https://doi.org/10.1177/001316446002000116.

Keogh, S., Mills, G., Fealy, R., 2012. The energy budget of the urban surface: two locations in Dublin. Ir. Geogr. 45, 1–23. https://doi.org/10.1080/00750778.2012.689182.

Landauer, M., Juhola, S., Klein, J., 2018. The role of scale in integrating climate change adaptation and mitigation in cities, 62, pp. 741–765. https://doi.org/10.1080/09640568.2018.1430022.

Li, X.X., Zhou, Y., Asrar, G.R., Imhoff, M., Li, X.X., 2017. The surface urban heat island response to urban expansion: a panel analysis for the conterminous United States. Sci. Total Environ. 605–606, 426–435. https://doi.org/10.1016/j.scitotenv.2017.06.229.

Mallen, E., Stone, B., Lanza, K., 2019. A methodological assessment of extreme heat mortality modeling and heat vulnerability mapping in Dallas, Texas. Urban Clim. 30, 100528. https://doi.org/10.1016/j.uclim.2019.100528.

Maragno, D., Dalla Fontana, M., Musco, F., 2020. Mapping heat stress vulnerability and risk assessment at the neighborhood scale to drive urban adaptation planning. Sustainability 12, 1056. https://doi.org/10.3390/su12031056.

Méndez-Lázaro, P., Muller-Karger, F.E., Otis, D., McCarthy, M.J., Rodríguez, E., 2018. A heat vulnerability index to improve urban public health management in San Juan, Puerto Rico. Int. J. Biometeorol. 62, 709–722. https://doi.org/10.1007/s00484-017-1319-z.

Nardo, M., Saisana, M., Saltelli, A., Tarantola, S., Hoffman, A., Giovannini, E., 2005. Handbook on constructing composite indicators: methodology and user guide. In: OECD Statistics Working Papers, 2005/03. OECD Publishing, Paris. https://doi.org/10.1787/9789264043466-en.

Navarro-Estupiñan, J., Robles-Morua, A., Díaz-Caravantes, R., Vivoni, E.R., 2019. Heat risk mapping through spatial analysis of remotely-sensed data and socioeconomic vulnerability in Hermosillo. México. https://doi.org/10.1016/j.uclim.2019.100576.

Nayak, S.G., Shrestha, S., Kinney, P.L., Ross, Z., Sheridan, S.C., Pantea, C.I., Hsu, W.H., Muscatiello, N., Hwang, S.A., 2018. Development of a heat vulnerability index for New York State. Public Health 161, 1–11. https://doi.org/10.1016/j.puhe.2017.09.006.

Nolan, P., 2015. Ensemble of Regional Climate Model Projections for Ireland. Environ. Prot, Agency.

Nolan, P., Flanagan, J., 2020. High-Resolution Climate Projections for Ireland-A Multi-Model Ensemble Approach (Dublin).

Oke, T.R., 1982. The energetic basis of the urban heat island. Q. J. R. Meteorol. Soc. 108, 1–24. https://doi.org/10.1002/qj.49710845502.

Oke, T.R., Mills, G., Christen, A., Voogt, J.A., 2017. Urban Climates. Cambridge University Press.

O'Malley, P.G., 2007. Heat waves and heat-related illness: preparing for the increasing influence of climate on health in temperate areas. J. Am. Med. Assoc. https://doi.org/10.1001/jama.298.8.917.

Oppenheimer, M., Campos, M., Warren, R., Birkmann, J., Luber, G., O'Neill, B., Takahashi, K., 2014. IPCC-WGII-AR5–19. Emergent Risks and Key Vulnerabilities. Clim. Chang. 2014 Impacts, Adapt. Vulnerability. Part A Glob. Sect. Asp. Contrib. Work. Gr. II to Fifth Assess. Rep. Intergov. Panel Clim. Chang, pp. 1039–1099.

Pappenberger, F., Jendritzky, G., Staiger, H., Dutra, E., Di Giuseppe, F., Richardson, D.S., Cloke, H.L., 2015. Global forecasting of thermal health hazards: the skill of probabilistic predictions of the universal thermal climate index (UTCI). Int. J. Biometeorol. 59, 311–323. https://doi.org/10.1007/s00484-014-0843-3.

Paranunzio, R., Ceola, S., Laio, F., Montanari, A., 2019. Evaluating the effects of urbanization evolution on air temperature trends using nightlight satellite data. Atmosphere (Basel). 10 https://doi.org/10.3390/atmos10030117.

Paranunzio, R., O'Dwyer, B., Alexander, P.J., Guerrini, M., Dwyer, N., Gault, J., 2020. Assessing Vulnerability to Climate Change : An Approach Illustrated through Large Urban Scale Adaptation (Urb-ADAPT). Dublin.

Pascal, M., Corso, M., Chanel, O., Declercq, C., Badaloni, C., Cesaroni, G., Henschel, S., Meister, K., Haluza, D., Martin-Olmedo, P., Medina, S., 2013. Assessing the public health impacts of urban air pollution in 25 European cities: results of the Aphekom project. Sci. Total Environ. 449, 390–400. https://doi.org/10.1016/j.scitotenv.2013.01.077.

Paterson, S.K., Godsmark, C.N., 2020. Heat-health vulnerability in temperate climates: lessons and response options from Ireland. Glob. Health 16, 1–17. https://doi.org/10.1186/s12992-020-00554-7.

Peng, S., Piao, S., Ciais, P., Friedlingstein, P., Ottle, C., Bréon, F.M., Nan, H., Zhou, L., Myneni, R.B., 2012. Surface urban heat island across 419 global big cities. Environ. Sci. Technol. 46, 696–703. https://doi.org/10.1021/es2030438.

Pobal, 2019. Pobal Maps Portal - by Compass Informatics [WWW Document]. URL. https://maps.pobal.ie/ (accessed 1.22.19).

Rafael, S., Martins, H., Marta-Almeida, M., Sá, E., Coelho, S., Rocha, A., Borrego, C., Lopes, M., 2017. Quantification and mapping of urban fluxes under climate change: application of WRF-SUEWS model to greater Porto area (Portugal). Environ. Res. 155, 321–334. https://doi.org/10.1016/j.envres.2017.02.033.

Reid, C.E., O'Neill, M.S., Gronlund, C.J., Brines, S.J., Brown, D.G., Diez-Roux, A.V., Schwartz, J., 2009. Mapping community determinants of heat vulnerability. Environ. Health Perspect. 117, 1730–1736. https://doi.org/10.1289/ehp.0900683.

Reid, C.E., Mann, J.K., Alfasso, R., English, P.B., King, G.C., Lincoln, R.A., Margolis, H.G., Rubado, D.J., Sabato, J.E., West, N.L., Woods, B., Navarro, K.M., Balmes, J. R., 2012. Evaluation of a heat vulnerability index on abnormally hot days: an environmental public health tracking study. Environ. Health Perspect. 120, 715–720. https://doi.org/10.1289/ehp.1103766.

Robine, J.M., Cheung, S.L.K., Le Roy, S., Van Oyen, H., Griffiths, C., Michel, J.P., Herrmann, F.R., 2008. Death toll exceeded 70,000 in Europe during the summer of 2003. Comptes Rendus - Biol. 331, 171–178. https://doi.org/10.1016/j.crvi.2007.12.001.

Rød, J.K., Berthling, I., Lein, H., Lujala, P., Vatne, G., Bye, L.M., 2012. Integrated Vulnerability Mapping for Wards in Mid- Norway 9839. https://doi.org/10.1080/13549839.2012.685879.

Sabrin, S., Karimi, M., Fahad, M.G.R., Nazari, R., 2020. Quantifying environmental and social vulnerability: role of urban Heat Island and air quality, a case study of Camden, NJ. Urban Clim. 34, 100699. https://doi.org/10.1016/j.uclim.2020.100699.

Santamouris, M., 2020. Recent progress on urban overheating and heat island research. Integrated assessment of the energy, environmental, vulnerability and health impact. Synergies with the global climate change. Energy Build. https://doi.org/10.1016/j.enbuild.2019.109482.

Savić, S., Marković, V., Šećerov, I., Pavić, D., Arsenović, D., Milošević, D., Dolinaj, D., Nagy, I., Pantelić, M., 2018. Heat wave risk assessment and mapping in urban areas: case study for a midsized central European city, Novi Sad (Serbia). Nat. Hazards 91, 891–911. https://doi.org/10.1007/s11069-017-3160-4.

Schatz, J., Kucharik, C.J., 2015. Urban climate effects on extreme temperatures in Madison, Wisconsin, USA. Environ. Res. Lett. 10, 094024 https://doi.org/10.1088/1748-9326/10/9/094024.

Schmidtlein, M.C., Deutsch, R.C., Piegorsch, W.W., Cutter, S.L., 2008. A sensitivity analysis of the social vulnerability index. Risk Anal. 28, 1099–1114. https://doi.org/10.1111/j.1539-6924.2008.01072.x.

Stewart, I.D., Oke, T.R., 2012. Local climate zones for urban temperature studies. Bull. Am. Meteorol. Soc. 93, 1879–1900. https://doi.org/10.1175/BAMS-D-11-00019.1.

Stone, B., Mallen, E., Rajput, M., Broadbent, A., Krayenhoff, E.S., Augenbroe, G., Georgescu, M., 2021. Climate change and infrastructure risk: indoor heat exposure during a concurrent heat wave and blackout event in Phoenix, Arizona. Urban Clim. 36, 100787. https://doi.org/10.1016/j.uclim.2021.100787.

Sweeney, J., 1987. The Urban Heat Island of Dublin City. Ir. Geogr. 20, 1–10. https://doi.org/10.1080/00750778709478819.

Taylor, K.E., Stouffer, R.J., Meehl, G.A., 2012. An overview of CMIP5 and the experiment design. Bull. Am. Meteorol. Soc. 93, 485–498. https://doi.org/10.1175/BAMS-D-11-00094.1.

Theeuwes, N.E., Ronda, R.J., Harman, I.N., Christen, A., Grimmond, C.S.B., 2019. Parametrizing horizontally-averaged wind and temperature profiles in the urban roughness sublayer. Boundary-Layer Meteorol. 321–348. https://doi.org/10.1007/S10546-019-00472-1, 2019 1733 173.

Verdonck, M.L., Demuzere, M., Hooyberghs, H., Beck, C., Cyrys, J., Schneider, A., Dewulf, R., Van Coillie, F., 2018. The potential of local climate zones maps as a heat stress assessment tool, supported by simulated air temperature data. Landsc. Urban Plan. 178, 183–197. https://doi.org/10.1016/j.landurbplan.2018.06.004.

Verdonck, M.L., Demuzere, M., Hooyberghs, H., Priem, F., Van Coillie, F., 2019. Heat risk assessment for the Brussels capital region under different urban planning and greenhouse gas emission scenarios. J. Environ. Manag. 249 https://doi.org/10.1016/j.jenvman.2019.06.111.

WHO, 2019. Health Impact Assessment (HIA) [WWW Document]. URL. https://www.who.int/teams/environment-climate-change-and-health/air-quality-and-health/hia-tools-and-methods/using-evidence-within-hia (accessed 3.12.21).

WHO, W.H.O, 2004. Heat-Waves: Risks and Responses. Heal. Glob. Environ. Heal. Ser. No.2, p. 124. https://doi.org/10.1007/s00484-009-0283-7.

Wolf, T., McGregor, G., Wolf, Tanja, McGregor, Glenn Russel, Wolf, T., McGregor, G., Tanja Wolf, G.R.M., Wolf, T., McGregor, G., 2013. The development of a heat wave vulnerability index for London, United Kingdom. Weather Clim. Extrem. 1, 59–68. https://doi.org/10.1016/j.wace.2013.07.004.

Working Groups I II III, IPCC, 2014. Climate Change 2014 Synthesis Report. Ipcc Ar5 1–112. https://doi.org/10.1017/CBO9781107415324.

Zhao, L., Lee, X., Smith, R.B., Oleson, K., 2014. Strong contributions of local background climate to urban heat islands. Nature 511, 216.

Zhou, Y., Smith, S.J., Zhao, K., Imhoff, M., Thomson, A., Bond-Lamberty, B., Asrar, G.R., Zhang, X., He, C., Elvidge, C.D., 2015. A global map of urban extent from nightlights. Environ. Res. Lett. 10, 054011 https://doi.org/10.1088/1748-9326/10/5/054011.